Testing of Full-Scale Two-Story Steel Plate Shear Wall with Reduced Beam Section Connections and Composite Floors

Bing Qu, S.M.ASCE[1]; Michel Bruneau, M.ASCE[2]; Chih-Han Lin[3]; and Keh-Chyuan Tsai[4]

Abstract: A two-phase experimental program was generated on a full-scale two-story steel plate shear wall with reduced beam section connections and composite floors, to experimentally address the replaceability of infill panels following an earthquake and the seismic behavior of the intermediate beam. In Phase I, the specimen was pseudodynamically tested, subjected to three ground motions of progressively decreasing intensity. The buckled panels were replaced by new panels prior to submitting the specimen to a subsequent pseudodynamic test and cyclic test to failure in Phase II. It is shown that the repaired specimen can survive and dissipate significant amounts of hysteretic energy in a subsequent earthquake without severe damage to the boundary frame or overall strength degradation. It is also found that the specimen had exceptional redundancy and exhibited stable force-displacement behavior up to the story drifts of 5.2 and 5.0% at the first and second story, respectively. Experimental results from pseudodynamic and cyclic tests are compared to seismic performance predictions obtained from a dual strip model using tension only strips and from a monotonic pushover analysis using a three-dimensional finite-element model, respectively, and good agreement is observed.

DOI: 10.1061/(ASCE)0733-9445(2008)134:3(364)

CE Database subject headings: Shear walls; Steel plates; Replacement; Cyclic tests; Seismic design; Pseudodynamic method.

Introduction

A steel plate shear wall (SPSW) consists of infill steel panels surrounded by boundary beams and columns. These panels are allowed to buckle in shear and subsequently form a diagonal tension field. SPSWs are progressively being used as the primary lateral force resisting systems in buildings (Sabelli and Bruneau 2006). Past monotonic, cyclic, and shaking table tests on SPSW in the United States, Canada, Japan, Taiwan, and other countries have shown that this type of structural system can exhibit high initial stiffness, behave in a ductile manner, and dissipate significant amounts of hysteretic energy, which make it a suitable option for the design of new buildings as well as for the retrofit of existing constructions (extensive literature reviews are available in Sabelli and Bruneau 2006; Berman and Bruneau 2003a, to name a few). Analytical research on SPSW has also validated useful models for the design and analysis of this lateral load resisting system (Thorburn et al. 1983; Elgaaly et al. 1993; Driver et al. 1997; Berman and Bruneau 2003b). Recent design procedures for SPSW are provided by the CSA "Limit states design of steel structures" (CSA 2003) and the AISC *Seismic Provision for Structural Steel Buildings* (AISC 2005). Innovative SPSW designs have also been proposed and experimentally validated to expand the range of applicability of SPSW (Berman and Bruneau 2003a,b; Vian and Bruneau 2005).

However, some impediments still exist that may limit the widespread acceptance of this structural system. For example, no research has directly addressed the replaceability of infill steel panels following an earthquake, and there remain uncertainties regarding the seismic behavior of intermediate beams in SPSW (intermediate beams are those to which steel plates are welded above and below, by opposition to top and bottom beams that have steel plates only below or above, respectively). The latter problem was analytically addressed by Lopez Garcia and Bruneau (2006) using simple models, but experimental investigations on the behavior of intermediate beams, particularly for beams having reduced beam section (RBS) connections and composite concrete slabs, can provide much needed information on the behavior of this structural system and how to best design the intermediate beams.

To address the above issues with regard to SPSW performance, a two-phase experimental program was developed to test a two-story SPSW specimen having an intermediate composite beam with RBS connections. The testing program also investigated how to replace a steel panel after a severe earthquake and how the repaired SPSW would behave in a second earthquake. This paper summarizes the tests conducted, observed ultimate behavior, and adequacy of simple models to replicate the global behavior of the SPSW considered.

[1]Ph.D. Candidate, Dept. of Civil, Structural and Environmental Engineering, 206 Ketter Hall, Univ. at Buffalo, Buffalo, NY 14260 (corresponding author). E-mail: bingqu@buffalo.edu

[2]Director, Multidisciplinary Center for Earthquake Engineering Research; and, Professor, Dept. of Civil, Structural and Environmental Engineering, Univ. at Buffalo, Buffalo, NY 14260. E-mail: bruneau@buffalo.edu

[3]Assistant Research Fellow, National Center for Research on Earthquake Engineering, 200, Sec. 3, Xinhai Rd., Taipei 106, Taiwan. E-mail: hanklin@ncree.org

[4]Director, National Center for Research on Earthquake Engineering and Professor, Dept. of Civil Engineering, National Taiwan Univ., 200, Sec. 3, Xinhai Rd., Taipei 106, Taiwan. E-mail: kctsai@ncree.org

Note. Associate Editor: Scott A. Civjan. Discussion open until August 1, 2008. Separate discussions must be submitted for individual papers. To extend the closing date by one month, a written request must be filed with the ASCE Managing Editor. The manuscript for this paper was submitted for review and possible publication on January 18, 2007; approved on July 5, 2007. This paper is part of the ***Journal of Structural Engineering***, Vol. 134, No. 3, March 1, 2008. ©ASCE, ISSN 0733-9445/2008/3-364–373/$25.00.

Specimen Description Test Setup and Instrumentation

A full-scale two-story one-bay SPSW specimen was designed and fabricated in Taiwan and a two-phase experimental program (Phase I and II tests) was conducted at the laboratory of the National Center for Research on Earthquake Engineering (NCREE) in Taipei, Taiwan.

The specimen, with equal height and width panels at each story, was 8,000 mm high (4,000 mm at each story) and 4,000 mm wide, measured between boundary frame member centerlines. The infill panels and boundary frame members were sized based on the recommendations provided by Berman and Bruneau (2003b). Beams and columns were of A572 Grade 50 steel members. Infill panels were specified to be SS400 steel, which is similar to ASTM A36 steel (Kuan 2005). H532 × 314 × 25 × 40 columns were used at each story. H446 × 302 × 13 × 21, H350 × 252 × 11 × 19, and H458 × 306 × 17 × 27 beams were employed at the top, intermediate, and bottom levels, respectively. The names of Taiwan designation H shapes (corresponding to United States designation W shapes) reflect their depth, flange width, as well as web and flange thicknesses. The RBS connection design procedure of Federal Emergency Management Agency (FEMA) Document, FEMA 350 (FEMA 2000) was used to detail the beam-to-column connections at the top, intermediate, and bottom levels, respectively. This detail was designed to ensure all inelastic beam action would occur at these locations. Composite slabs, having a 3W-0.92t corrugated steel deck per Taiwan designation equivalent to a 3 in. composite gauge 20 deck (James River Steel 2004), were designed to be 150 mm thick from the top of the composite slab to the bottom flute and 2,480 mm wide at floor levels.

In Phase I tests, the infill panels were 3 and 2 mm thick with measured yield strength of 335 and 338 MPa at the first and second story, respectively. Prior to Phase II tests, the buckled infill panels were removed using flame cut and replaced by 3.2- and 2.3-mm-thick new panels with measured yield strength of 310 and 285 MPa at the first and second story, respectively. Measured differences are within tolerances for such plates and steel grade. Fish plates with thickness of 6 mm and height of 70 mm were used along the boundary frame members to connect infill panels. The infill panels of Phase I were welded on one side of the fish plates and the new panels installed as part of Phase II were welded on the other side (after Phase I panels were cut out). The specimen was not straightened between tests. In the Phase I tests, the infill panels were restrained by horizontal restrainers for the sole purpose of minimizing the amplitude of the out-of-plane displacements of the panels that typically develop in SPSW at large inelastic story drifts. According to the restrainer design procedure proposed by Lin et al. (2006), rectangular tubes of 125 × 75 × 4 and 125 × 75 × 2.3 were placed at quarter points of the first and second story, respectively. The names of Taiwan designation rectangular tubes (corresponding to United States designation rectangular HHS) reflect their depth, width, as well as wall thickness. No restrainers were utilized in Phase II tests. The specimen is shown schematically in Fig. 1. This paper principally focuses on the Phase II tests as these specimens are more representative of North American practice.

The specimen was mounted on the strong floor. In-plane (north-south) servo controlled hydraulic actuators were mounted between the specimen and a reaction wall. Based on the ultimate strength of the specimen assessed using plastic analysis procedures (Berman and Bruneau 2003b), three 1,000 kN hydraulic

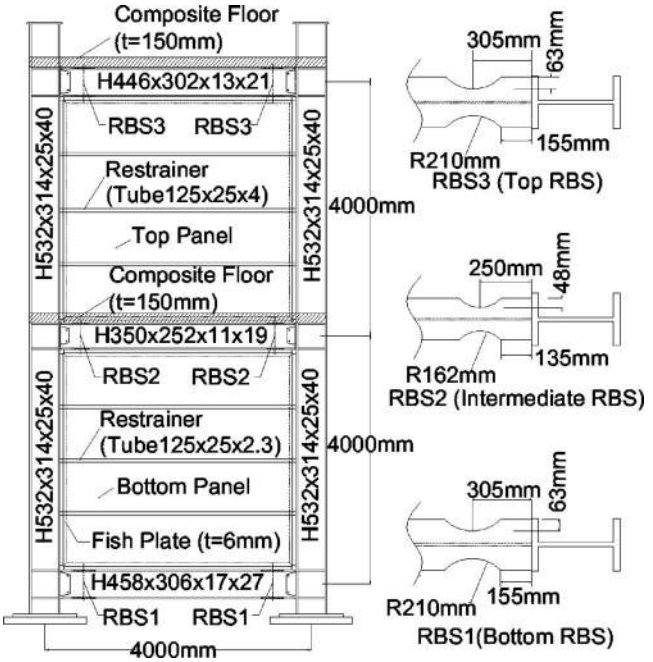

Fig. 1. Schematic of specimen

actuators were employed to apply earthquake load or cyclic load on the specimen at each story. Ancillary trusses (as part of the floor slab system) were used to transfer in-plane loads to the specimen at the floor levels. In order to avoid out-of-plane (east-west) displacements of the SPSW at floor levels, two hydraulic actuators were mounted at each floor level between the edge of the floor (ancillary truss) and a reaction frame. A vertical load of 1,400 kN was applied by a reaction beam at the top of each column to simulate gravity load that would be present in the prototype. Each reaction beam transferred the load exerted from two vertical actuators mounted between the reaction beam and anchor rods pinned to the strong floor. The test setup is illustrated in Figs. 2(a and b).

Instrumentation consisted of strain gauges mounted on the boundary frame. Uniaxial strain gauges were placed at quarter points of the story height on the flange of each column. Rosette strain gauges were placed at 1/4 and 3/4 points of the story height on the web of each column (one on each side of the web) so that the principal stress could be obtained.

Tiltmeters were placed at various locations on every beam and column to obtain in-plane rotations of these parts. Dial meters were placed at each column base to monitor the relative displacement between the column bases and strong floor resulting from possible slippage of the specimen on the strong floor under in-plane loading.

Magnetostrictive transducers (Temposonics) were placed at the north ends of the intermediate and top beams, respectively, to obtain the story drift histories during the tests.

Based on the preliminary strip model of the SPSW specimen, linearly variable displacement transformers (LVDTs) were placed across the panels at an angle of 41° from the vertical to obtain the diagonal elongation of the infill panels (12 LVDTs for each story, i.e., six on each side of the infill panel).

PI gauges were placed at the panel zones of intermediate and bottom beam-to-column connections, respectively, to obtain the deformation of these parts. A total of 203 channels were used to collect experimental data. More information about the instrumen-

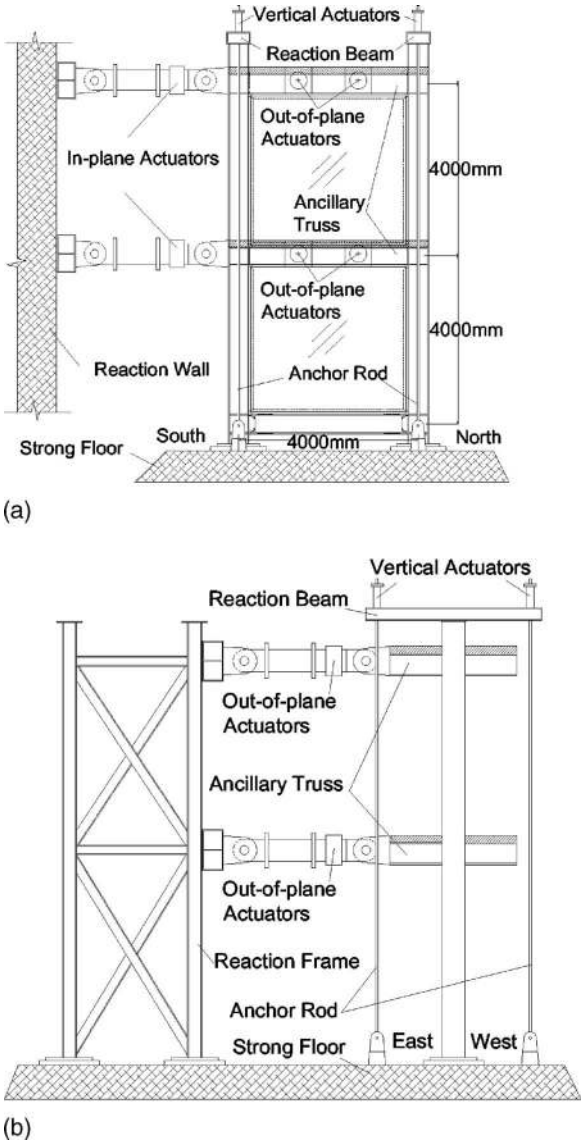

Fig. 2. (a)-(b) Test setup

tation is provided elsewhere (Tsai et al. 2006; Qu and Bruneau 2008). Five video cameras were used to record the global behavior of the specimen and the local behaviors of RBS connections and infill panels.

Phase I Tests

In order to investigate the seismic behavior of SPSW in severe earthquake and aftershocks, the specimen was tested under three pseudodynamic loads using the Chi-Chi earthquake record (TCU082EW) scaled up to levels of excitations representative of seismic hazards having 2, 10, and 50% probabilities of exceedances in 50 years, subjecting the wall to earthquakes of progressively decreasing intensity. The ground accelerations were scaled so that the spectral acceleration (5% damping) associated with the first mode period (0.52 s) was equal to that in the design response spectra. Despite the numerous ancillary calculations that checked the adequacy of the specimen, the intermediate concrete slab suffered premature cracks and two anchor bolts fractured at the south column base at time steps of 9.5 and 24 s of the first earthquake

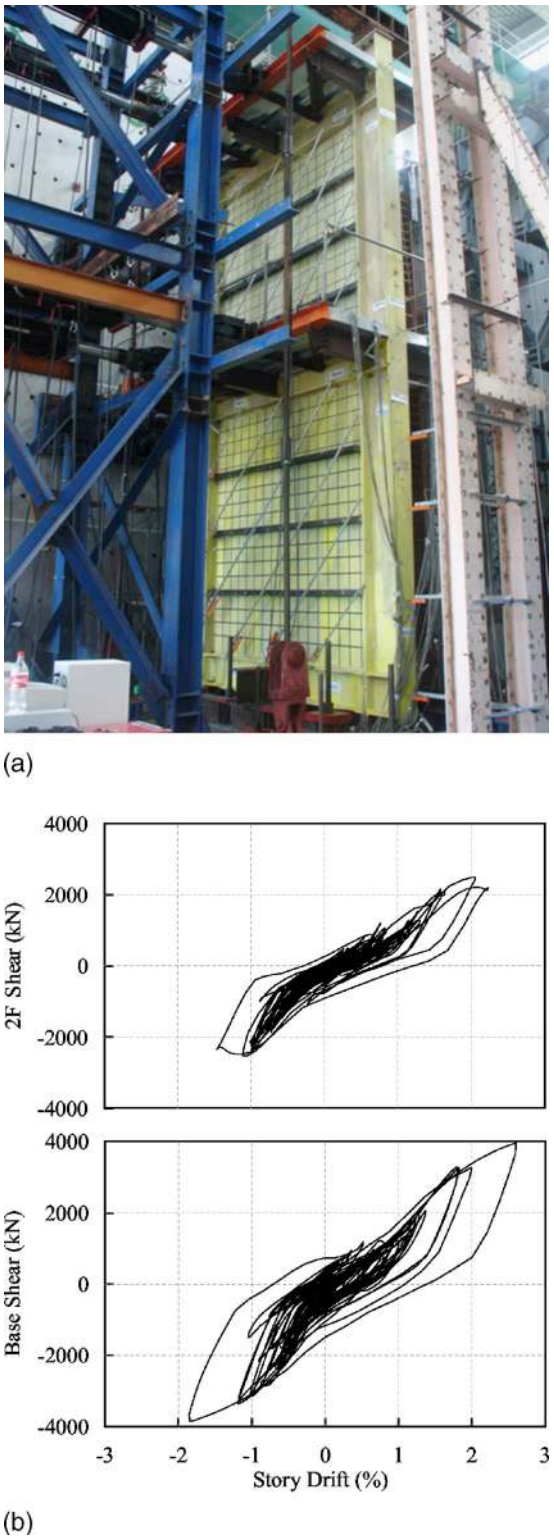

Fig. 3. Specimen and hystereses of first pseudodynamic test of phase I: (a) specimen prior to Phase I tests; (b) hystereses

record, respectively. The tests resumed after the specimen load transfer mechanisms were strengthened at those locations.

The SPSW behaved similarly to the Phase II pseudodynamic test described in greater length below. The infill panels dissipated energy and buckled as anticipated, with maximum amplitude of out-of-plane deformations of 50 mm. The residual story drifts were 0.31 and 0.29% at the first and second story, respectively, at

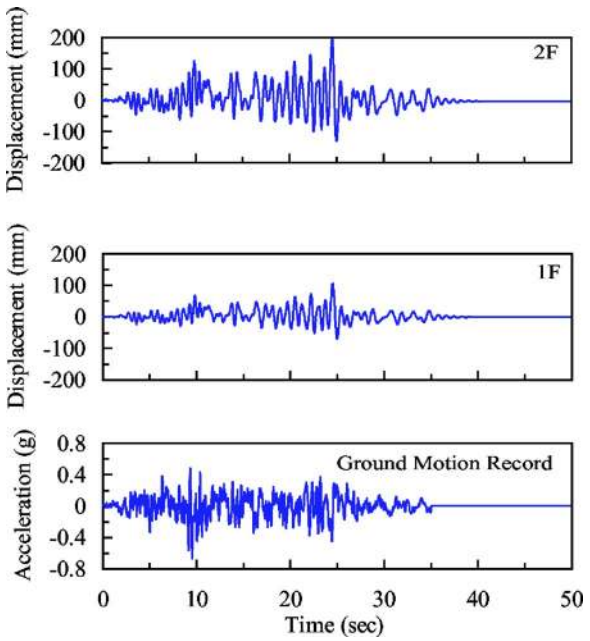

Fig. 4. Ground motion record and displacement histories

the end of the Phase I tests. No fracture was found in the boundary frame, and it was deemed to be in satisfactory condition, allowing for the replacement of infill panels for the subsequent phase of testing. The global responses corresponding to the first earthquake record as well as the specimen prior to testing are summarized in Figs. 3(a and b). Story drifts designated as "+" or "−" refer to loading in the north and south direction (pushing away from or pulling towards the reaction wall), respectively. Detailed information about specimen design and results from the Phase I tests are presented elsewhere (Lin et al. 2006, 2007).

Phase II Pseudodynamic Test

As mentioned in the descriptions of the specimen, the buckled panels were replaced by new panels before submitting the SPSW specimen to further testing. It took a crew of three technicians 2- 1/2 days to complete the infill panel replacement.

In order to investigate how the repaired SPSW specimen would behave in a second earthquake in the first stage of Phase II, the specimen was tested under pseudodynamic loads corresponding to the Chi-Chi earthquake record (TCU082EW) scaled to a seismic hazard having a 2% probability of occurrence in 50 years (i.e., equivalent to the first earthquake record considered in the Phase I tests). This scaled earthquake record had a peak ground acceleration (PGA) of 0.63g and the peak pseudoacceleration (PSA) response of 1.85g at the fundamental period of 0.52 s. The original ground motion record and the displacement histories at floor levels are shown in Fig. 4. Note that loud noise was heard as the infill panels buckled during the test.

The SPSW specimen and hysteretic curves obtained from the Phase II pseudodynamic test, along with the counterpart results obtained from Phase I for a similar level of excitation are shown in Figs. 5(a and b). Observation of the hysteretic curves obtained from Phase II shows that the first story dissipated more hysteretic energy than the second story. The infill panels buckled over both stories as anticipated, with maximum amplitude of out-of-plane deformations of 250 mm. Both the first and second story exhibited stable force-displacement behavior, with some pinching of the hysteretic loops as the magnitude of story drifts increased, particularly after the development of a small fracture along the bottom of the shear tab at the north end of the intermediate beam at story drifts of 2.6 and 2.3% at the first and second story, respectively. After the pseudodynamic test, the boundary frame was in good condition (except for the aforementioned damage in the

(a)

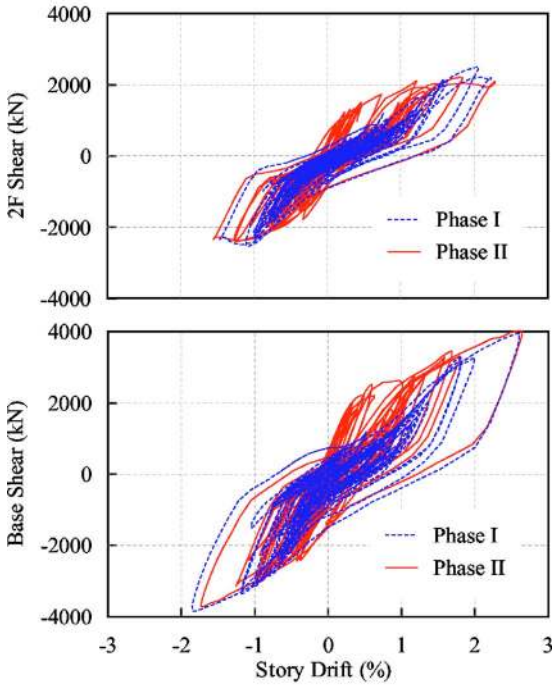

(b)

Fig. 5. Specimen and hystereses: (a) specimen prior to Phase II tests; (b) hystereses of Phase I and Phase II

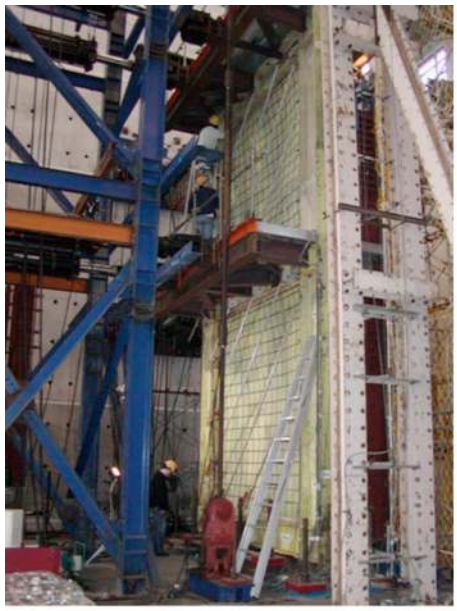

(a)

(c)

(b)

Fig. 6. Deformed specimen and buckled panels in Phase II pseudodynamic test: (a) specimen; (b) 1F panel; and (c) 2F panel

shear tab of the intermediate beam). There were notable plastic deformations at the column bases and RBS connections at all levels. Small fractures were found at the panel corners. All welds within the SPSW specimen were intact after the test. The deformed specimen and buckled panels after the Phase II pseudodynamic test are shown in Figs. 6(a–c) respectively.

Comparing the hysteretic curves from the Phase I and Phase II tests shown together in Fig. 5(b), the two specimens are found to behave similarly under the same strong ground motion except that the initial stiffness of the repaired specimen is higher than that of the original one. This is because the results shown for the specimen in Phase I are those obtained after the specimen was repaired due to the unexpected failures mentioned earlier. Therefore the infill panels had already experienced some inelastic deformation before these unexpected failures occurred.

Analytical Modeling of Phase II Pseudodynamic Test

To check the adequacy of the strip model to predict the nonlinear behavior of SPSW under the Phase II pseudodynamic load, a dual strip model using tension-only strips was developed using the commercially available finite-element software package ABAQUS/Standard. Thirty strips (15 strips in each direction) were used at each story as shown in Fig. 7(a). The boundary frame was fixed at column bases to replicate the test conditions. Boundary conditions preventing out-of-plane displacements were imposed at floor levels. Gravity loads were first applied at the top of the columns. Then the displacement histories obtained from the test were used as displacement input at floor levels.

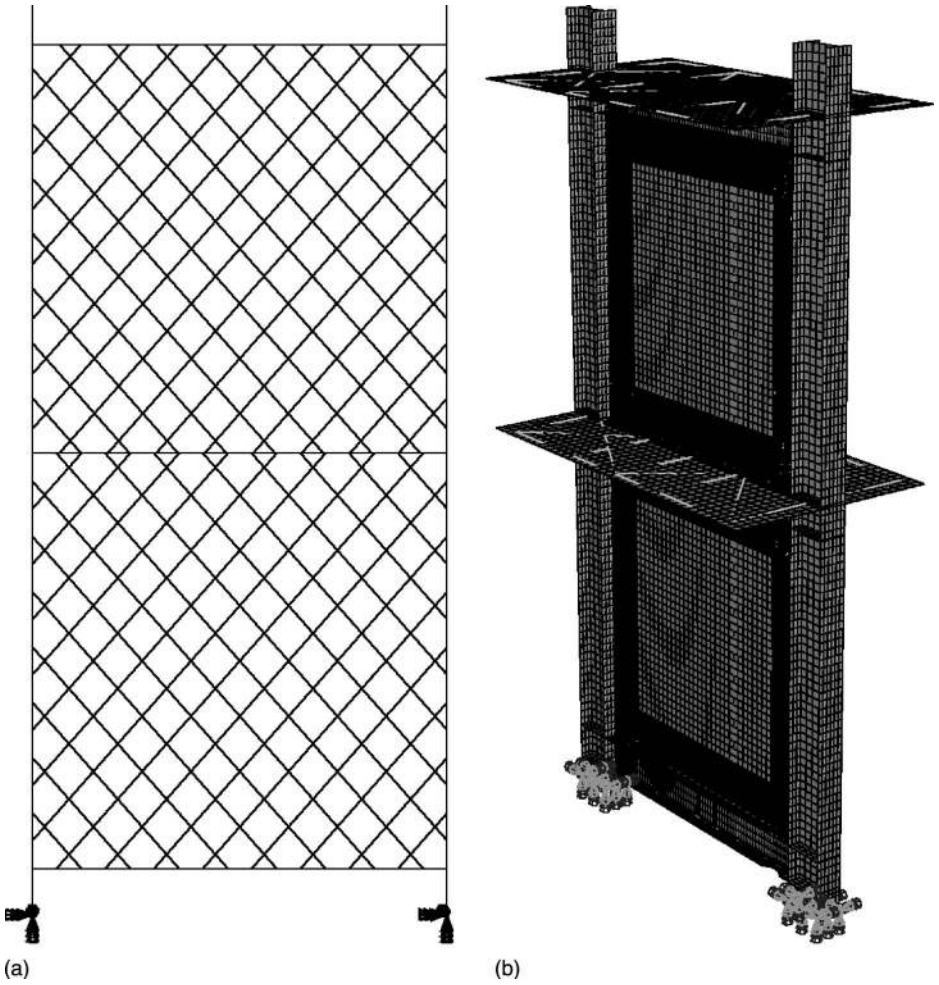

Fig. 7. Analytical models: (a) dual strip model; (b) 3D FE model

The arc cutouts of the RBS connections were simplified as rectangular cutoffs for the purpose of this analysis. The length and width of the approximate reduced beam flange using rectangular cutoffs were equal to the length and minimum width of the original reduced beam flange, respectively, recognizing that this is a somewhat more severe reduction than the actual RBS used.

To consider the contribution of the concrete slabs to the global behavior of the SPSW specimen, the thicknesses of the top flanges of the intermediate and top beam were increased to provide the same positive plastic section moment capacity as the real composite beam section. Composite action was neglected in negative flexure.

Beam elements (ABAQUS Element B31) and truss elements (ABAQUS Element T3D2) were used to represent the boundary frame and dual strips, respectively. B31 is a two-node three-dimensional (3D) linear beam element which allows biaxial bending, axial strain and transverse shear deformations. T3D2 is a two-node 3D linear truss element.

Nominal stress-strain curves for the infill panels as well as the boundary frame members were obtained from coupon tests. Steel was modeled as an isotropic material with a simple elastoplastic constitutive behavior. Von Mises yield surface was adopted as the yield criterion for the boundary frame members with identical strengths in tension and compression. Tension-only strength was given to the diagonal strips.

The hysteretic curves obtained from the above dual strip model are plotted on top of those experimentally obtained from the Phase II pseudodynamic test in Fig. 8. It is found that the global behavior of the SPSW specimen can be satisfactorily predicted by the dual strip model.

Phase II Cyclic Testing to Failure

The next stage of the Phase II tests involved the cyclic test of the SPSW specimen to investigate the ultimate behavior of the intermediate beam and the cyclic behavior and ultimate capacity of the SPSW.

As mentioned earlier, the boundary frame members were still in good condition after the pseudodynamic test, except for a small visible fracture along the bottom of the shear tab at the north end of the intermediate beam. To correct this limited damage and get a better assessment of the possible ultimate capacity of SPSW, the damaged shear tab was replaced by a new one prior to conducting the cyclic test.

A displacement-controlled scheme was selected for the cyclic test. Because the first mode response dominated the global response of the SPSW in the prior pseudodynamic test (although some higher mode effects were observed) and to allow testing both panels even if failure progressively develops at one of the

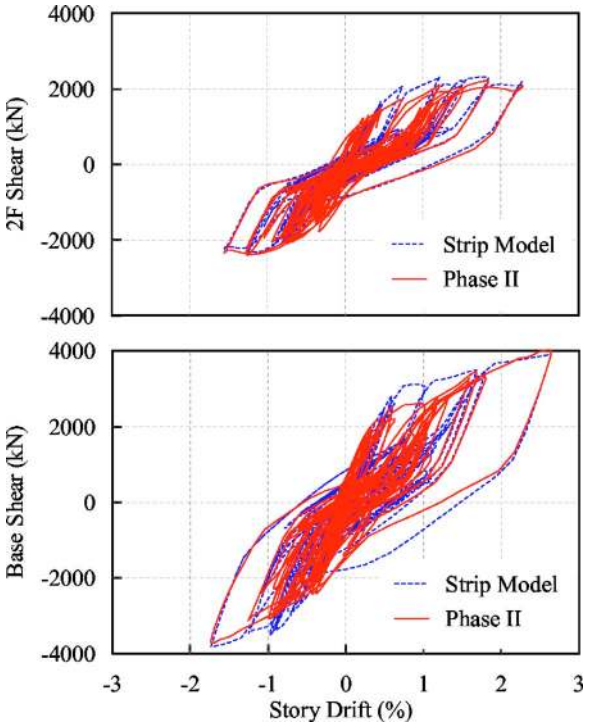

Fig. 8. Hystereses from strip model and Phase II pseudodynamic test

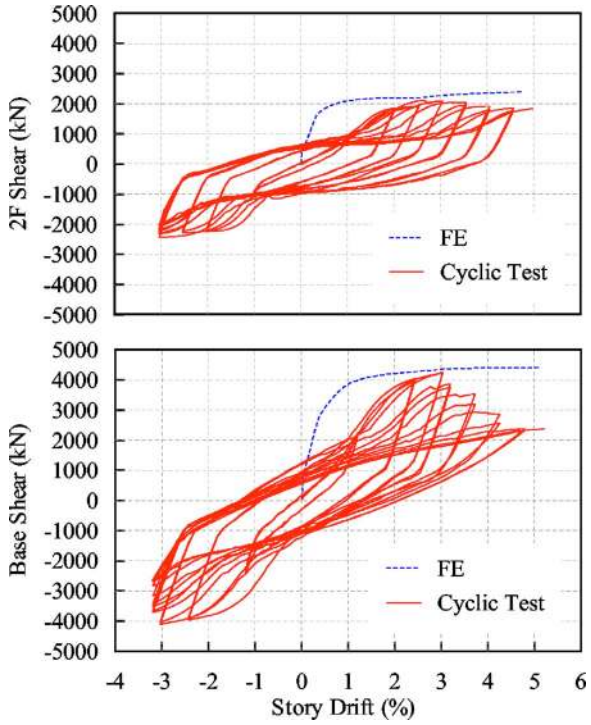

Fig. 9. Monotonic pushover curves and hystereses of Phase II cyclic test

two stories, a displacement constraint was exerted to keep the in-plane actuators displacing in a ratio corresponding to a first mode of response throughout the entire test. Table 1 shows the story drift history of the first and second story, respectively. Since the specimen was pulled (to the south) to the maximum actuator stroke when peak story drifts reached −3.2 and −3.0% at the first and second story, respectively, the applied displacement history became unsymmetrical beyond that point, in that the peak story drifts due to loading toward the south were kept at −3.2 and −3.0% at the first and second story, respectively, in all subsequent cycles while increasing displacements were still applied in the other direction.

The hysteretic curves resulting from the Phase II cyclic test, along with the results of a monotonic pushover analysis described in detail in the next section, are shown in Fig. 9. Comparing the hysteretic curves in Fig. 9 to those in Fig. 5(b), it is observed that the initial stiffness of the SPSW specimen in the cyclic test was smaller than that in pseudodynamic test. Because the previous pseudodynamic test stretched the infill panels up to specimen story drifts of 2.6 and 2.3% at the first and second story, respectively, the hysteretic loops exhibited pinching up to those story drifts. Hysteretic loops were then full until story drifts of 2.8 and 2.6% at the first and second story, respectively, in Cycle 7, when complete fracture occurred along the shear tab at the north end of the intermediate beam. This unexpected failure resulted in story shear reductions of 76 and 83 kN at the first and second story, respectively, mainly because the test was being conducted under displacement control rather than force control. A similar fracture developed along the shear tab at the south end of the intermediate beam when the specimen was pulled towards the reaction wall in this cycle.

Rupture of the shear tabs triggered fracture of the bottom flange at the north end of the intermediate beam. At story drifts of 3.3 and 3.1% at the first and second story, respectively, in Cycle 9, the bottom flange at the north end of the intermediate beam

Table 1. Cyclic Story Drift Histories

			1F		2F	
Displacement step	Number of cycles	Cumulative number of cycles	Positive drift (%)	Negative drift (%)	Positive drift (%)	Negative drift (%)
1	2	2	1.2	−1.2	1.0	−1.0
2	2	4	2.4	−2.4	2.0	−2.0
3	2	6	3.0	−3.0	2.5	−2.5
4	2	8	3.2	−3.2	3.0	−3.0
5	2	10	3.7	−3.2	4.5	−3.5
6	2	12	4.3	−3.2	4.0	−3.0
7	2	14	4.8	−3.2	4.5	−3.0
8	0.25	14.25	5.2	—[a]	5.0	—[a]

[a]Not applicable.

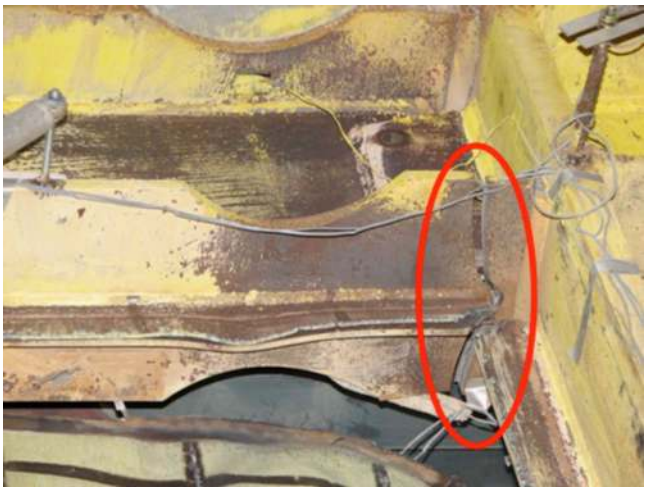

Fig. 10. Ruptures at north end of intermediate beam

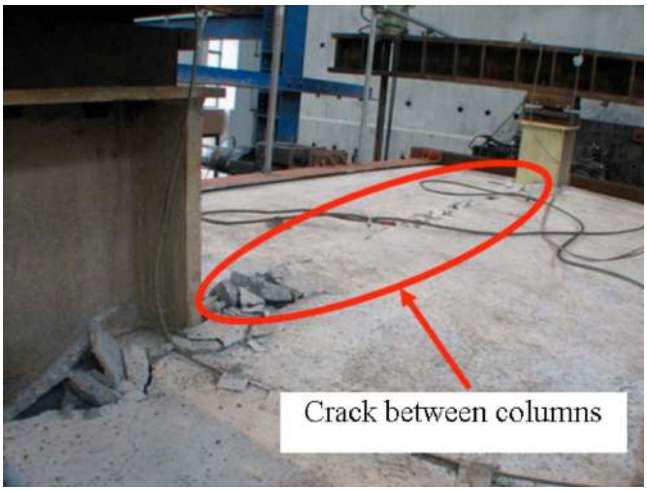

Fig. 12. Crack at top slab

fractured as shown in Fig. 10. However, no fractures developed in the reduced beam flange regions of the intermediate beam. The welds connecting the infill panels to the fish plates around the north end of the intermediate beam also fractured over a substantial length to a more severe extent after the specimen experienced story drifts of 5.2 and 5.0% at the first and second story, respectively, as shown in Fig. 11. These events significantly changed the load path within the system. However, the SPSW specimen was still able to exhibit stable force-displacement behavior as evidenced by the hysteretic curves shown in Fig. 9, which demonstrates the redundancy of this kind of structural system. It is unclear at this time how much of this redundancy is attributable to the composite floor and ancillary truss, or the panels and boundary frame.

The cyclic test ended at story drifts of 5.2 and 5.0% at the first and second story, respectively, when sudden failure occurred in the load transfer mechanism, i.e., when a fatal longitudinal crack developed along the top concrete slab of the specimen, as shown in Fig. 12.

Fig. 11. Fractures of welds connecting infill panels to fish plates

Analytical Modeling of Phase II Cyclic Test

To further assess the global behavior of the SPSW specimen, a 3D finite-element (FE) model as shown in Fig. 7(b) was developed in ABAQUS/Standard to simulate the responses of the specimen subjected to the Phase II cyclic test. Vian and Bruneau (2005) demonstrated that although the entire cyclic response of SPSW can be replicated using such finite-element models, the monotonic response obtained from a pushover analysis using such a model can adequately capture the global behavior of a SPSW at the peak story drifts of a cyclic test—hence only monotonic analysis was conducted here.

Shell elements (ABAQUS Element S4R) were employed for all structural subassemblages. S4R is a four-node, quadrilateral shell element with reduced integration and a large-strain formulation. A total of 30,553 elements were used for this model. The boundary frame was fixed at column bases. Boundary conditions preventing out-of-plane displacements were used along the intermediate and top concrete slab, respectively. Gravity loads were applied at the top of the columns prior to the in-plane loading. Lateral in-plane displacements were applied at the floor levels in proportion to the same ratio used in the test.

Nominal stress-strain curves for all steel structural subassemblages were obtained from the coupon test. Steel was modeled as an isotropic material with a simple elastoplastic constitutive behavior. Von Mises yield surface was selected as the yield criterion. In this case, the actual concrete slab was modeled using an unconfined concrete model and the compressive strength measured from cylinder tests.

Linear eigenvalue buckling analysis was performed prior to the monotonic pushover analysis to introduce initial imperfections in the panel, and ensure reliable modeling of their buckling. The

global structural response from this finite-element simulation was compared with the experimental results from the cyclic test, as shown in Fig. 9.

It is observed that the story shears from the FE analysis are greater than those obtained from the cyclic test prior to 2.6 and 2.3% story drifts at the first and second story, respectively. This is principally because the specimen was loaded into the inelastic range in the prior Phase II pseudodynamic test, resulting in the partial absence of tension field in the infill panel at low story drift levels. However, the story shears obtained from FE analysis fit well those obtained from the cyclic test at story drifts exceeding the maximum story drifts of 2.6 and 2.3% at the first and second story, respectively, reached in the Phase II pseudodynamic test. After story drifts of 3 and 2.5% at the first and second story, respectively, the story shears from cyclic tests are smaller than those from FE analysis due to the ruptures in the intermediate beam and failures of the welds connecting infill panels to fish plates.

Conclusions

A full-scale two-story SPSW specimen with RBS connections and composite floors was designed and subjected to pseudodynamic and cyclic testing, to experimentally address the replaceability of infill panels following an earthquake, as well as the behavior of the repaired SPSW in a subsequent earthquake and the seismic performance of the intermediate beam.

The pseudodynamic tests show that a SPSW repaired by replacing the infill panels buckled in a prior earthquake by new ones can be a viable option to provide adequate resistance to the lateral loads imparted on this structure during new seismic excitations (note that possible undesirable aesthetic issues related to residual story drifts from the first earthquake prior to repair are beyond the scope of this work). The repaired SPSW behaved quite similarly to the original one. Testing showed that the repaired SPSW can survive and dissipate a similar amount of energy in the subsequent earthquake without severe damage to the boundary frame and without overall strength degradation.

Results from the cyclic test allow us to investigate the ultimate displacement capacity of the SPSW specimen. Although the hysteretic curves were pinched at the low story drift levels due to the inelastic deformations that the infill panels experienced during the pseudodynamic test, and even though the strength of the SPSW dropped as the ends of the intermediate beam fractured, the SPSW structure exhibited stable force-displacement behavior and provided a significant energy dissipation capacity, exhibiting substantial redundancy.

The adequacy of the dual strip model using tension-only strips was found accurate to predict the nonlinear behavior of SPSW under earthquake load, as demonstrated by comparison with the experimental results of the Phase II pseudodynamic test. The ultimate lateral in-plane load capacity of SPSW was shown to be equally well predicted by a monotonic pushover analysis using a 3D FE model with shell elements, when comparing with the experimental results from the Phase II cyclic test.

The columns and anchor beams, as well as top and bottom RBS connections performed as intended. However, the intermediate beam failed unexpectedly. The ends of the intermediate beam having RBS connections ultimately developed fractures in the shear tabs followed by fractures at the end of the bottom beam flanges. No fractures developed in the reduced beam flange region. Further investigation is required to clarify the local behavior of the intermediate beam in SPSW, to develop a better understanding of how such an intermediate beam should be designed.

Acknowledgments

This work was financially supported in part by the Taiwan National Science Council and the Taiwan National Center for Research on Earthquake Engineering, and in part by the Earthquake Engineering Research Centers Program of the US National Science Foundation under Award No. ECC-9701471 to the Multidisciplinary Center for Earthquake Engineering Research. All sponsors are gratefully acknowledged. The writers are also grateful to China Steel, who provided the construction materials for the specimens, and to the technical support at NCREE. Any opinions, findings, conclusions, and recommendations presented in this paper are those of the writers and do not necessarily reflect the views of the sponsors.

References

AISC. (2005). *Seismic provisions for structural steel buildings*, Chicago.

Berman, J. W., and Bruneau, M. (2003a). "Experimental investigation of light-gauge steel plate shear walls for the seismic retrofit of buildings." *Technical Rep. No. MCEER-03-0001*, Multidisciplinary Center for Earthquake Engineering Research, Buffalo, N.Y.

Berman, J. W., and Bruneau, M. (2003b). "Plastic analysis and design of steel plate shear walls." *J. Struct. Eng.*, 129(11), 1448–1456.

Canadian Standards Association (CSA). (2003). "Limit states design of steel structures." *CAN/CSA S16-01*, Willowdale, Ontario.

Driver, R. G., Kulak, G. L., Kennedy, D. J. L., and Elwi, A. E. (1997). "Seismic behavior of steel plate shear walls." *Structural Engineering Rep. No. 215*, Univ. of Alberta, Edmonton, Alberta, Canada.

Elgaaly, M., Caccese, V., and Du, C. (1993). "Postbuckling behavior of steel-plate shear walls under cyclic loads." *J. Struct. Eng.*, 119(2), 588–605.

Federal Emergency Management Agency (FEMA). (2000). "Recommended seismic design criteria for new steel moment-frame buildings." *Rep. No. FEMA 350 Prepared by the SAC Joint Venture for FEMA*, Washington, D.C.

James River Steel Inc. (2004). "Composite floor decks." ⟨http://www.jamesriversteel.com/comp3.htm⟩.

Kuan, M. L. (2005). "Discussion on ASTM A36 and CNS SS400." ⟨http://www.twce.org.tw/info/%A7%DE%AEv%B3%F8/367-3-1.htm⟩ (in Chinese).

Lin, C. H., Tsai, K. C., Lin, Y. C., Wang, K. J., Hsieh, W. D., Weng, Y. T., Qu, B., and Bruneau, M. (2006). "The substructural pseudodynamic tests of a full-scale two-story steel plate shear wall." *Proc., 4th Int. Conf. on Earthquake Engineering*. Taipei, Taiwan, Paper No. 155.

Lin, C. H., Tsai, K. C., Lin, Y. C., Wang, K. J., Qu, B., and Bruneau, M. (2007). "Full scale steel plate shear wall: NCREE/MCEER phase I tests." *Proc., 9th Canadian Conf. on Earthquake Engineering*, Ottawa.

Lopez-Garcia, D., and Bruneau, M. (2006). "Seismic behavior of intermediate beams in steel plate shear walls." *Proc., 8th U.S. National Conf. on Earthquake Engineering*, San Francisco, Paper No. 1089.

Qu, B., and Bruneau, M. (2008). "Seismic behavior and ductile design of steel plate shear wall." *Technical Rep. No. MCEER-08-0010*, Multidisciplinary Center for Earthquake Engineering Research, Buffalo, N.Y., in press.

Sabelli, R., and Bruneau, M. (2006). *Steel plate shear walls (AISC design guide)*, American Institute of Steel Construction, Chicago.

Thorburn, L. J., Kulak, G. L., and Montgomery, C. J. (1983). "Analysis

of steel plate shear walls." *Structural Engineering Rep. No. 107*, Dept. of Civil Engineering, Univ. of Alberta, Edmonton, Alberta, Canada.
Tsai, K. C., Lin, C. H., Lin, Y. C., Hsieh, W. D., and Qu, B. (2006). "Substructural hybrid tests of a full scale two-story steel plate shear wall." *Technical Rep. No. NCREE-06-017*, National Center for Research on Earthquake Engineering, Taipei, Taiwan (in Chinese).
Vian, D., and Bruneau, M. (2005). "Steel plate shear walls for seismic design and retrofit of building structure." *Technical Rep. No. MCEER-05-0010*, Multidisciplinary Center for Earthquake Engineering Research, Buffalo, N.Y.